Anti-lung cancer targets of ellagic acid and biological interaction with a blood carrier protein

Xuru Jin [a,1], Junlei Ying [b,1], Jiangwei Ni [c], Zichen Gao [b], Xiang Zhang [c,*]

[a] Department of Respiratory and Critical Care Medicine, The First Affiliated Hospital of Wenzhou Medical University, Wenzhou, Zhejiang Province 325000, China
[b] Wenzhou Medical University, Wenzhou, Zhejiang Province 325000, China
[c] Department of Thoracic Surgery, The First Affiliated Hospital of Wenzhou Medical University, Wenzhou, Zhejiang Province 325000, China

ARTICLE INFO

ABSTRACT

Ellagic acid ($C_{14}H_6O_8$, 4,4′,5,5′6,6′-hexahydroxydiphenic acid 2,6,2′6′-dilactone) as a metabolite polyphenol compound has shown potential anticancer activities. However, its potential interaction affinity with plasma carrier proteins and antimetastatic activities are still unknown. Therefore, in this study, the anticancer and antimetastatic activities of ellagic acid in H358 metastatic lung cancer cells were assessed by MTT, qRT-PCR and western blotting. Then, the interaction of ellagic acid with human transferrin (HTf) as a drug carrier protein was measured. The results showed that ellagic acid-triggered cytotoxicity in H358 metastatic cells with an IC_{50} concentration of 7.18 μM. was mediated by overexpression of Bax/Bcl-2 ratio and caspase-3 mRNA as well as caspase-3 activity. Additionally, after being incubated with ellagic acid, the mRNA and protein expression levels of vascular endothelial growth factor (VEGF), a hallmark of angiogenesis, and the metastasis markers matrix metalloproteinase-2 (MMP-2) and MMP-9 were noticeably reduced. In protein–ligand interaction section, we found that one molecule of ellagic acid potentially binds to one molecule of HTf mediated by the involvement of hydrogen bonds and van der Waals forces, supported by molecular docking simulations. In conclusion, our novel data suggested that ellagic acid can show promising antimetastatic activity against H358 lung cancer cells as well as ideal binding affinity to a drug carrier protein model.

1. Introduction

The drug–plasma protein interaction plays a crucial role in drug pharmacodynamics and pharmacokinetics through affecting their bio-absorption, bio-distribution, bio-metabolism, and excretion characteristics (Schmidt et al., 2010, Fan et al., 2022). Furthermore, the therapeutic drug efficacy is associated with a potential balance between their bound and free fractions following interaction with blood proteins. As a result, investigations on the interaction of drugs with plasma proteins can provide us with useful details of the structural characteristics influencing the therapeutic potency of drugs (Yanget al., 2006, Haider et al., 2012). Therefore, exploring the interaction of proteins and drugs for determination of binding affinity and binding forces as well as structural changes of proteins has received great attention within different bio-/medical-related fields (Shahraki et al., 2023), which could serve as a reference for the analysis of different drugs in biological systems (Wang et al., 2022).

Ellagic acid ($C_{14}H_6O_8$, 4,4′,5,5′6,6′-hexahydroxydiphenic acid 2,6,2′6′-dilactone) as a metabolite polyphenol compound, presented in several medicinal plants and vegetables, including woody plants and grapes as well as nuts (Talcott and Lee, 2002) has shown different pharmacological activities (Losso et al., 2004, Ríos et al., 2018, Lu et al., 2023). For example, ellagic acid shows potential antioxidant, antibacterial, antidiabetic, anti-inflammatory, antiaging as well as anticancer activities (Zhu et al., 2022, Ahmadi and Javid, 2023, Zhang et al., 2023). Although potential anticancer activity of ellagic acid have been reported, there is still a room to elucidate the functional mechanism of ellagic acid on lung tumor growth and metastasis as a one of the most prevalent types of cancers in China (Nie et al., 2023). In fact, due to its rising prevalence and high mortality, lung cancer poses a serious threat to the public's health and places a tremendous burden on Chinese society (Wu et al., 2021).

Human transferrin (HTf, a monomeric 80-kDa glycoprotein with 679 amino acid residues) as the most abundant serum protein serves as a

* Corresponding author.
  E-mail address: Xiangzhang.12@outlook.com (X. Zhang).
[1] Equal contribution.

great candidate in the transporting of different drugs/compounds (Sarzehi and Chamani, 2010). Around half of the total (14 g) HTf is circulated in the blood plasma (Sarzehi and Chamani, 2010). Additionally, HTf contributes to the storage, transport and homeostasis of iron in vertebrates (Gkouvatsos et al., 2012).

The interaction mechanisms of several drugs such as temsirolimus (Shamsi et al., 2018), cyclophosphamide (Tousi et al., 2011), rivastigmine tartrate (Shamsi et al., 2019), and fluxoridin (Shahraki et al., 2024) with HTf have been investigated by different molecular docking and spectroscopic approaches. Then, it has been shown that small molecules as drugs can establish strong interaction with HTf deduced by different hydrophobic or hydrophilic interactions. The binding mechanism of small molecules with HTf further evaluated by molecular docking studies have revealed the properties of HTf binding pocket at atomic level.

As, the interaction of anticancer drugs to serum proteins is of a great importance in their potency due to the dramatic influences exerted on the circulation and bio-availability, in this paper, the interaction mechanisms of ellagic acid and HTf and metastatic lung cancer cell line were investigated by different biochemical, theoretical and cellular measurements.

2. Materials and methods

2.1. Materials

All reagents were of analytical grade and purchased from Merck Company (Darmstadt, Germany). Human apo-transferrin (HTf, CAS No.:11096-37-0), ellagic acid (CAS No.:476-66-4), dimethyl sulfoxide (DMSO), Roswell Park Memorial Institute-1640 (RPMI-1640) medium, and thiazolyl blue tetrazolium blue (MTT) were obtained from Sigma-Aldrich Company (St. Louis, MO, USA). Fetal bovine serum (FBS) was ordered from Invitrogen (Carlsbad, CA, USA). The HTf solution (1.25×10^{-6} M) was prepared in 50 mM phosphate buffer (pH 7.4). An ellagic acid solution (0.25×10^{-3} M) in a methanol/water (1:1, v/v) solution was also prepared (Zhang et al., 2020b). The HTf concentration was determined spectrophotometrically with an extinction coefficient of 32.183, 800 M^{-1} cm^{-1} at 280 nm (Santos et al., 2021). The concentration of ellagic acid was calculated spectrophotometrically at 260 nm with an extinction coefficient of 32.1 mL mg^{-1} cm^{-1} (Zhang et al., 2020b).

2.2. Cell culture

H358 metastatic lung cancer cells (Shanghai Cell Bank of Chinese Academy of Sciences) were grown in RPMI-160 medium containing 10 % FBS and 1 % penicillin/streptomycin and maintained at 37 °C with 5 % CO_2 in a humidified incubator.

2.3. MTT assay

The H358 metastatic lung cancer cells were used to assess the cytotoxicity of ellagic acid. Briefly, cells were seeded on 96-well plates a density of 1×10^4 cells per well and incubated for 24 h. Different concentrations of ellagic acid (1–100 μM) were then added to the cells and incubated for 24 h. Then, MTT solution (20 μL) was added to each well and incubated for 4 h at 37 °C. Afterward, the medium was replaced with DMSO (100 μL). Optical density of samples was read at 570 nm on a multiwell microplate reader (Synergy H1 Hybrid Multi-Mode Microplate Reader, BioTek).

2.4. Analysis of caspase-3 activity

Caspase-3 activity was assayed quantitatively using caspase-3 colorimetric assay kit (BioVision Research Products, CA, USA) as reported previously (Kaleem et al., 2016). Briefly, ~3×10^6 cells were resuspended with chilled lysis buffer, incubated on ice for 10 min, centrifuged (10,000g for 1 min), and added by 10 mM dithiothreitol (DTT) to the supernatant, and incubated for 30 min on ice. The samples were mixed with 50 μL of reaction buffer, added by 5 μL of 4 mM DEVD-pNA substrate, and incubated at 37 °C for 2 h. Absorbance of the samples was recorded at 405 nm on a multiwell microplate reader (Synergy H1 Hybrid Multi-Mode Microplate Reader, BioTek).

2.5. Quantitative real-time-PCR (qRT-PCR) analysis

Total RNA was extracted from cells using Trizol reagent (Invitrogen, USA), followed by reverse-transcription and amplification with the one-step RT-PCR System (TaKaRa, Dalian, China). Primer sequences of Bax, Bcl-2, caspase-3, MMP-2, MMP-9, and VEGF were designed as previously reported (Guruvayoorappan and Kuttan, 2008, Wu et al., 2016). PCR conditions was also done based on the previous report (Wohlkoenig et al., 2011). The level of β-actin gene expression was used as an internal control. The relative expression of target genes was expressed using the comparative $2^{-\Delta\Delta Ct}$ method.

2.6. Western blot analysis

H358 cells were seeded on 6-well plates a density of 1×10^6 cells per well followed by addition of fresh medium after 24 h with or without ellagic acid and further incubation for 24 h. Briefly, cell lysates were prepared and centrifuged (14,000 × g, 20 min) at 4 °C. Total protein concentrations were determined using Bradford assay kit (Sigma), and equal amounts (50 μg) of protein were subjected to polyacrylamide gels and transferred to nitrocellulose membranes. Specific proteins were detected with protein-specific antibodies [anti-matrix metalloproteinase 2 (MMP2) (ab92536), anti-MMP9 (ab283575), anti-vascular endothelial growth factor VEGFA (ab46154), and β-Actin (#4967, Cell Signaling Technology) at the manufacturer recommended dilutions. After washing, the membranes were incubated with secondary mouse anti-goat peroxidase conjugated antibodies (Cell Signaling Technologies) for 1 h at 37 °C. Enhanced chemiluminescence (ECL) detection reagent was used to detect proteins.

2.7. Tryptophan (Trp)/tyrosine (Tyr) fluorescence quenching

Trp/tyr fluorescence quenching were carried out on a fluorescence spectrometer (Lengguang F96 Shanghai, China), equipped with a 1-cm fluorescence cuvette. The emission spectra of HTF were read following an excitation wavelength of 280 nm. The Trp/tyr fluorescence spectra of HTf were obtained at four temperatures of 298 K, 303 K, 308 K, and 317 K and both excitation and emission slits were fixed to 5 nm. Titration experiments were manually done using a micropipette for the addition of ellagic acid solution to HTf solution. The solution of HTf (0.6 μM) was titrated with the addition of different concentrations of ellagic acid solution (0.6–21 μM). The fluorescence spectra were corrected against inner filter and dilution effects before further analyses (Ali et al., 2021).

2.8. Circular dichroism (CD) measurement

CD spectroscopy measurements were done using a J-1500CD Spectrometer (Jasco Instruments, Easton, MD). A solution of HTf (2.5 μM) was titrated by different HTf:ellagic acid molar ratios of (1:0, 1:1 1:10, and 1:35). The CD spectra of HTf were collected in the range of 260 nm to 200 nm at room temperature at a scanning speed of 100 nm/min. The contents of α-helix structures were analyzed by CDPro software package (Sreerama and Woody, 2000).

2.9. Molecular docking simulation

The structure of apo-HTf was retrieved from the RCSB Protein Data Bank with a PDB code of 2HAV. The ellagic acid structure ($C_{14}H_6O_8$ |
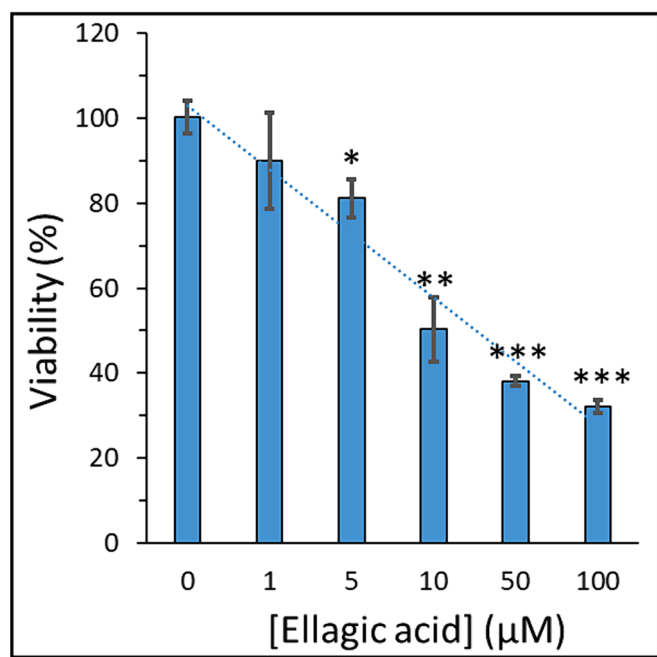
Fig. 1. Exploring the viability of H358 lung cancer cell line after exposure to varying concentrations of ellagic acid for 24, determined by MTT assay. Data are shown as mean ± SD of three experiments. *P < 0.05, **P < 0.01, ***P < 0.001.

CID ₅281855) was downloaded from https://pubchem.ncbi.nlm.nih.go v/compound/Ellagic-Acid. Molecular docking simulation was done using AutoDock Vina a search size of $136 \times 99 \times 107$ Å was used along with exhaustiveness criteria of 32. Ellagic acid was docked in a blind manner and10 independent docking runs were done. All poses were sorted and the lowest-energy conformations was selected.

2.10. Statistical analysis

Part of data are expressed as mean ± SD and significant differences between the groups were evaluated using the unpaired student's *t*-test. P < 0.05 was considered as an indication of statistical significance.

3. Results and discussion

3.1. Ellagic acid inhibits the growth of H358 lung cancer cell line

Our first aim in the cellular studies was to assess the influence of ellagic acid exposure on the cell viability of metastatic lung cancer cells. As a result, using H358 lung cancer cell line, we investigated the impact of different concentrations of ellagic acid on the proliferation of these cells by well-known MTT assay. It was exhibited that ellagic acid exposure to H358 lung cancer cell line led to a significant concentration-dependent inhibition of cell proliferation (Fig. 1). After incubation of H358 lung cancer cell line with 1, 5, 10, 50, and 100 μM of ellagic acid for 24 h, the cell viability decreased from 100 % to 100.33 % ±3.79 %, 90.07 %±11.34 %, 81.14 %±4.59 %, 50.28 %±7.57 %, 38.04 %±1.17 %, and 32.09 %±1.51 %, respectively.

The IC$_{50}$ value at 24 h treatment with ellagic acid for H358 lung cancer cell line was calculated to be 7.18 μM. It has been previously shown that the viability rates of A549 lung cancer cells significantly decreased by ellagic acid incubation in a concentration-dependent manner, relative to the control group. Liu et al. observed that at maximum studied concentration of 20 μM, more than 60 % of cells were still viable (Liu et al., 2018). These results in line with our data revealed that ellagic acid could significantly mitigate the viability of human A549 lung cancer cells (Liu et al., 2018). Additionally, Duan et al. reported

that incubation of lung adenocarcinoma cell lines HOP62 and H1975 with two concentrations of ellagic acid (25 and 50 μM) after 48 and 72 h resulted a significant reduction in cell viability, while HOP62 cells were more sensitive than H1975 cells to ellagic acid (Duan et al., 2019).

3.2. Ellagic acid induces apoptosis in H358 metastatic lung cancer cells

Apoptosis as a crucial signaling pathway for induction of cell death after incubation of cells with different kinds of drugs is typically regulated through the interaction of the Bcl-2 protein family (Tsujimoto and Shimizu, 2000). The mitochondrial pathway-mediated apoptosis which is generally relied on the Bcl-2 family of proteins typically lead to the effective release of cytochrome *C* as a pro-apoptotic factor from the mitochondria (Green, 2022, Qian et al., 2022). The Bcl-2 family of proteins is categorized into three groups of anti-apoptotic proteins (Bcl-2), pro-apoptotic members (Bax), and the BH3-only proteins (Bad) (Tsujimoto, 2003). Proteins that trigger or mitigate the induction of apoptosis can interact with each other and control the cell death or survival. Overexpression of Bax as well as downregulation of Bcl-2, enhances the sensitivity of cells to apoptotic stimuli which can lead to the activation of caspase proteins (Burlacu, 2003).

We evaluated the influence of ellagic acid on mRNA expression of Bax (Fig. 2A), Bcl-2 (Fig. 2B), ratio of Bax/Bcl-2 (Fig. 2C), and caspase-3 (Fig. 2D) in H358 metastatic lung cancer cells after 24 of incubation.

Results from qRT-PCR assay demonstrated a significant increase in the mRNA expression of Bax, ratio of Bax/Bcl-2 and caspase-3 accompanied by a significant reduction in the expression of Bcl-2 mRNA in H358 lung cancer cells after exposure to 7.18 μM (IC$_{50}$ concentration) ellagic acid (Fig. 2). Also, ellagic acid-treated H358 lung cancer cells exhibited increased caspase-3 activity, compared to control group (Fig. 2E). This data suggested that ellagic acid induced anticancer effects in H358 lung cancer cells through an apoptosis-mediated mechanism, which is in good agreement with previous studies (Lu et al., 2023). Generally, these results suggest that Bax, Bcl-2, and caspase-3 play a key role in controlling ellagic acid-stimulated apoptosis in H358 lung cancer cells. Previous studies have also shown that ellagic acid could regulate the proliferation of prostate cancer cell (Malik et al., 2011), HepG2 human hepatocellular carcinoma cell (Zhang et al., 2014), and HCT-15 colon adenocarcinoma cell (Umesalma et al., 2015) via Bax, Bcl-2 and caspase-3-mediated apoptosis signaling pathway.

3.3. Ellagic acid regulates metastatic characteristics of H358 lung cancer cells

Cancer metastasis is recognized to be characterized by both invasion and migration of cancer cells. Through metastasis, cancer cells usually intrude into blood vessels, transfer through the blood circulation, and reside in distant tissues (Majidpoor and Mortezaee, 2021). It has been shown that overexpression of MMP-2, MMP-9 and VEGF are heavily associated with proliferation, metastasis and angiogenesis of lung carcinoma (Guruvayoorappan and Kuttan, 2008, Balla et al., 2016).

Upregulation of MMP and VEGF could be involved in tumor metastasis. Upregulation of MMP-2, MMP-9 and VEFG have been reported in malignant tumor progression, mostly because MMPs are able to potentially degrade basement membrane's collagen, fibronectin, and gelatin (Guruvayoorappan and Kuttan, 2008).

Therefore, we assessed the expression of MMP-2 mRNA (Fig. 3A), MMP-9 mRNA (Fig. 3B) and VEGF mRNA (Fig. 3C) as well as their protein expression levels (Fig. 3D). MMP-2 and MMP-9 were used as metastatic markers and VEGF as an angiogenesis marker. Results showed a remarkable decrease in MMP-2, MMP-9 and VEGF mRNA and protein expression in ellagic acid-treated H358 lung cancer cells relative to control samples (Fig. 3), suggesting that ellagic acid downregulates the expression of metastatic and angiogenesis markers in lung cancer cells. Taken together, these outcomes indicated that ellagic acid is a promising candidate for control of metastatic lung cancer.
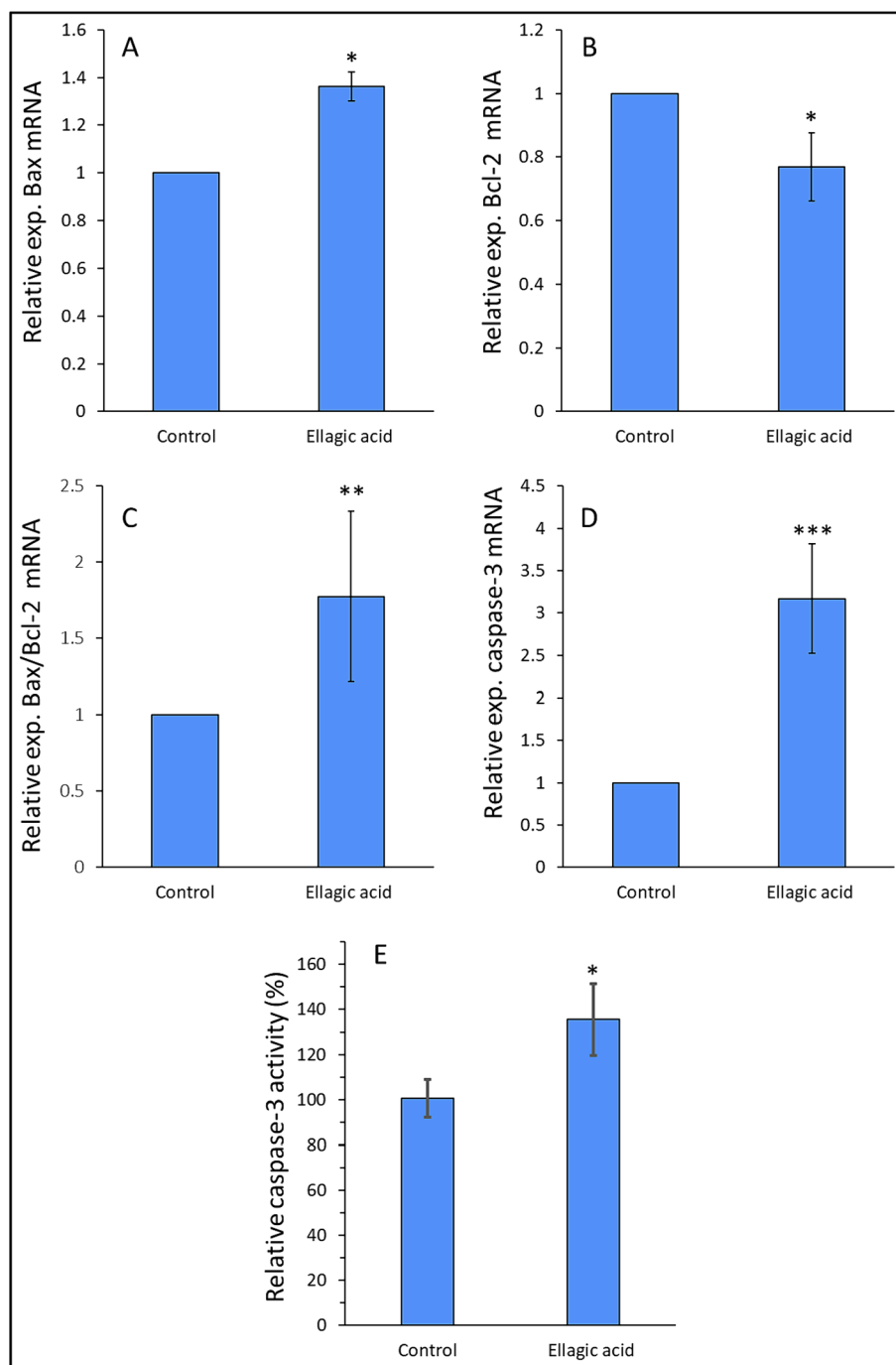
Fig. 2. Exploring the mRNA expression of Bax (A), Bcl-2 (B), Bax/Bcl-2 ratio (C), caspase-3 (D), and caspase-3 activity (E) of H358 lung cancer cell line after exposure to IC_{50} concentration of ellagic acid (7.18 μM) for 24, determined by qRT-PCR assay and enzyme assay. Data are shown as mean ± SD of three experiments. *$P <$ 0.05, **$P <$ 0.01, ***$P <$ 0.001.

3.4. Impact of ellagic acid on HTf fluorescence

The effect of ellagic acid on fluorescence intensity of HTf was shown in Fig. 4. The fluorescence emission intensity of HTf was reduced continuously with the increase of ellagic acid concentration.

It reveals that ellagic acid might potentially interact with HTf and serves as a quencher to reduce the fluorescence emission intensity of HTf. The fluorescence quenching of HTf was not blue or red shifted in the presence of ellagic acid (Fig. 4), suggesting that the polarity of HTf fluorophore micro-environment was not heavily changed upon the interaction with ellagic acid (Shakibapour et al., 2023).

3.5. Fluorescence quenching mechanisms

Static or dynamic fluorescence quenching process upon interaction of ligands and HTf is deduced from the formation of non-fluorescent ground state complex or collision quenching, respectively (Li et al., 2023, Shakibapour et al., 2023). To further analyze the kind of fluorescence quenching mechanism, the fluorescence quenching data at four temperatures of 298 K, 303 K, 308 K, and 317 K were analyzed by well-known Stern-Volmer (SV) equation (Khan et al., 2023):

$$F_0/F = K_{SV}[ellagic\,acid] + 1 = k_q \tau_0 [ellagic\,acid] + 1 \tag{1}$$
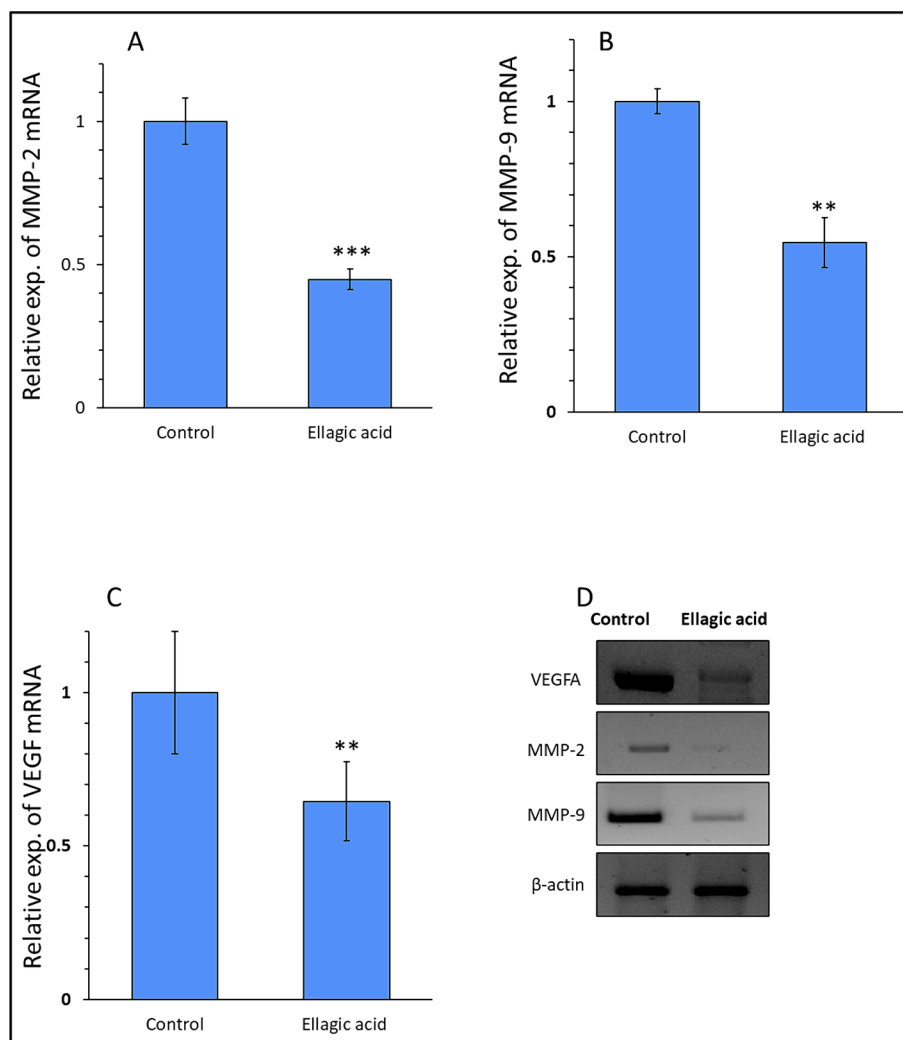
Fig. 3. Exploring the mRNA expression of MMP-2 (A), MMP-9 (B), VEGF (C), and protein expression of these markers (D) in H358 lung cancer cell line after exposure to IC_{50} concentration of ellagic acid (7.18 μM) for 24, determined by qRT-PCR and western blot. Data are shown as mean ± SD of three experiments. **P < 0.01, ***P < 0.001.

where F_0 and F are the fluorescence emission intensities of HTf and HTf-ellagic acid complex, respectively. K_{SV} is the SV quenching constant, k_q is the rate constant, τ_0 is a constant value of 7.208 ns (Li et al., 2023). The SV plots were displayed in Fig. 5 and the resultant K_{SV} and k_q values were summarized in Table 1.

Generally, K_{SV} values are inversely correlated with temperature for occurring a static quenching mechanism, whereas for dynamic quenching K_{SV} values are directly correlated with temperature (Li et al., 2023, Shamsi et al., 2023). Additionally, the k_q value of static quenching is typically greater than the limiting diffusion rate constant of the biomolecules, 2×10^{10} M^{-1} s^{-1} (Li et al., 2023). It can be deduced that a good linear relationship of the SV plots for HTf-ellagic acid system. Linear SV plots are normally associated with a single class of fluorophores in HTf which might equally accessible to ellagic acid, or reveal that only one kind of quenching mechanism (dynamic or static) is dominant (Li et al., 2023). As can be deduced from Table 1, the K_{SV} values were reduced with increasing temperature and the values of k_q were greater than 2×10^{10} M^{-1} s^{-1} for the ellagic acid-HTf systems, illustrating that the quenching mechanism of HTf by ellagic acid is only static quenching mechanism (Shamsi et al., 2023).

Generally, it can be indicated that linear SV plots were indicative of static quenching rather than combined static and dynamic or dynamic quenching for HTf-ellagic acid system (Li et al., 2023, Shamsi et al., 2023).

3.6. Binding parameters

The values of the binding constant (K_b) and the number of binding sites (n) upon interaction of HTf and ellagic acid can be calculated using the following equation (Shamsi et al., 2020b):

$$Log(F_0 - F/F) = LogK_b + n\log[ellagic acid] \tag{2}$$

where F_0, F have the same definition as in Eq. (1). The values of K_b and n calculated form Fig. 6 are summarized in Table 2.

The plots with good linearity are indicative of a site-binding model between ellagic acid and HTf. Therefore, we can conclude that a single class of binding sites on THf molecule is presented for ellagic acid. The binding affinities between ellagic acid and HTf at all four studied temperatures are all moderate based on the K_b values (10^4 M^{-1}). The K_b values of ellagic acid were reduced with the increase of temperature, suggesting that temperature rising declines the stability of HTf-ellagic acid system, and the binding reactions between ellagic acid and HTf is an exothermic process.

The K_b values are heavily assosiated with the presence of binding sites in the biomolecule as well as the bioaffinity of the small molecules to the receptor (Li et al., 2022). As the binding nature of ligand–protein is specific and based on the calculated K_b values in this study, we can
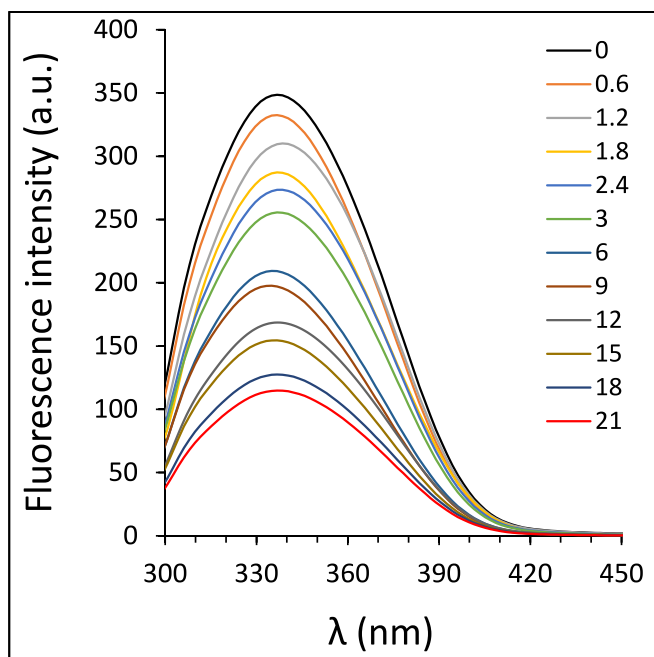
Fig. 4. Exploring the interaction of different concentrations of ellagic acid and HTf at 298 K, determined by fluorescence quenching study.
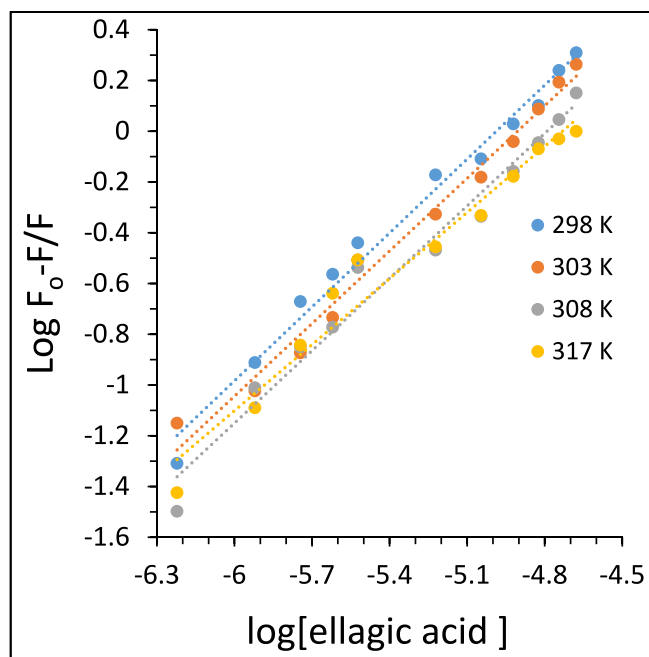
Fig. 6. Modified Stern-Volmer plots of the interaction of different concentrations of ellagic acid and HTf, determined by fluorescence quenching study.

Fig. 5. Stern-Volmer plots of the interaction of different concentrations of ellagic acid and HTf, determined by fluorescence quenching study.

Table 2
Binding parameters of HTf-ellagic acid system at different temperatures.

System	T (K)	logK$_b$	n	R^2
HTf-ellagic acid	298	4.84	0.97	0.9863
	303	4.67	0.95	0.9856
	308	4.55	0.95	0.9736
	317	4.10	0.86	0.9630
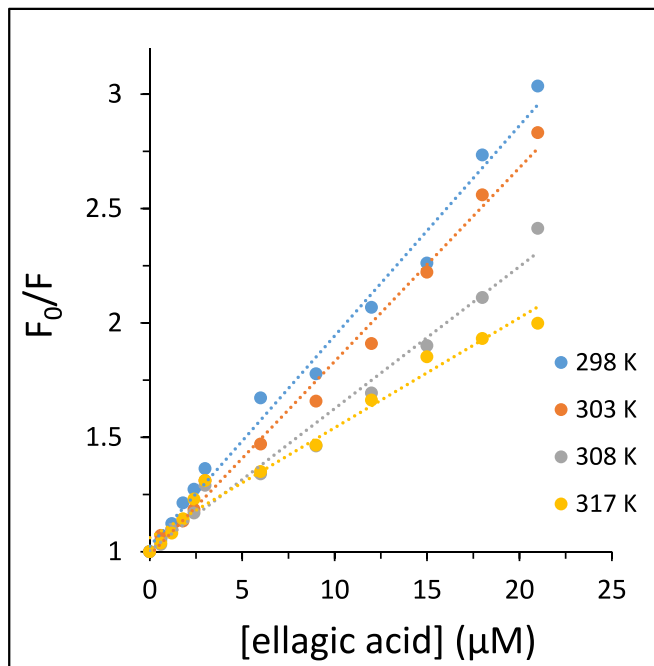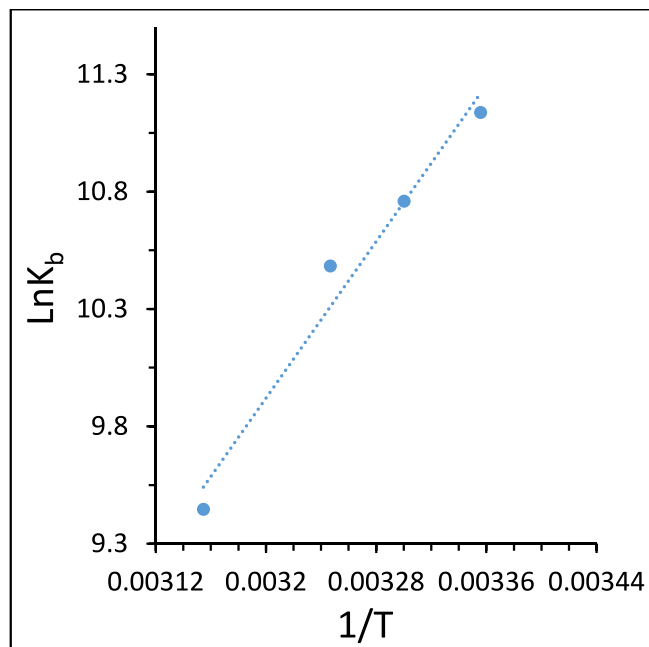
Fig. 7. Van' t Hoff plots of the interaction of ellagic acid and HTf, determined by fluorescence quenching study.

Table 1
K_{SV} and kq values for the interaction of HTf with ellagic acid at four different temperatures.

System	T (K)	K$_{SV}$ × 10^4 (M^{-1})	k$_q$ × 10^{13} (M^{-1} s^{-1})	R^2
HTf-ellagic acid	298	9.18	1.27	0.9892
	303	8.47	1.17	0.9926
	308	6.21	0.86	0.9836
	317	4.81	0.66	0.9764

Table 3

Thermodynamic parameters of HTf-ellagic acid system at different temperatures.

System	T (K)	ΔH (kJ/mol)	ΔS (J/mol K)	ΔG (kJ/mol)
HTf-ellagic acid	298	−69.22	−139.18	−27.74
	303			−27.05
	308			−26.35
	317			−25.10

interpret them as a particular characteristic between the ellagic acid and HTf. By comparing the K_b values obtained in our study with those determined in others studies for galantamine (Khan et al., 2021), cyanidin (Khashkhashi-Moghadam et al., 2022), and some flavonols (Li et al., 2023), we can conclude that the K_b values reflect a moderate affinity between ellagic acid and HTf.

3.7. Thermodynamic parameters and binding forces

Different thermodynamic parameters including enthalpy change
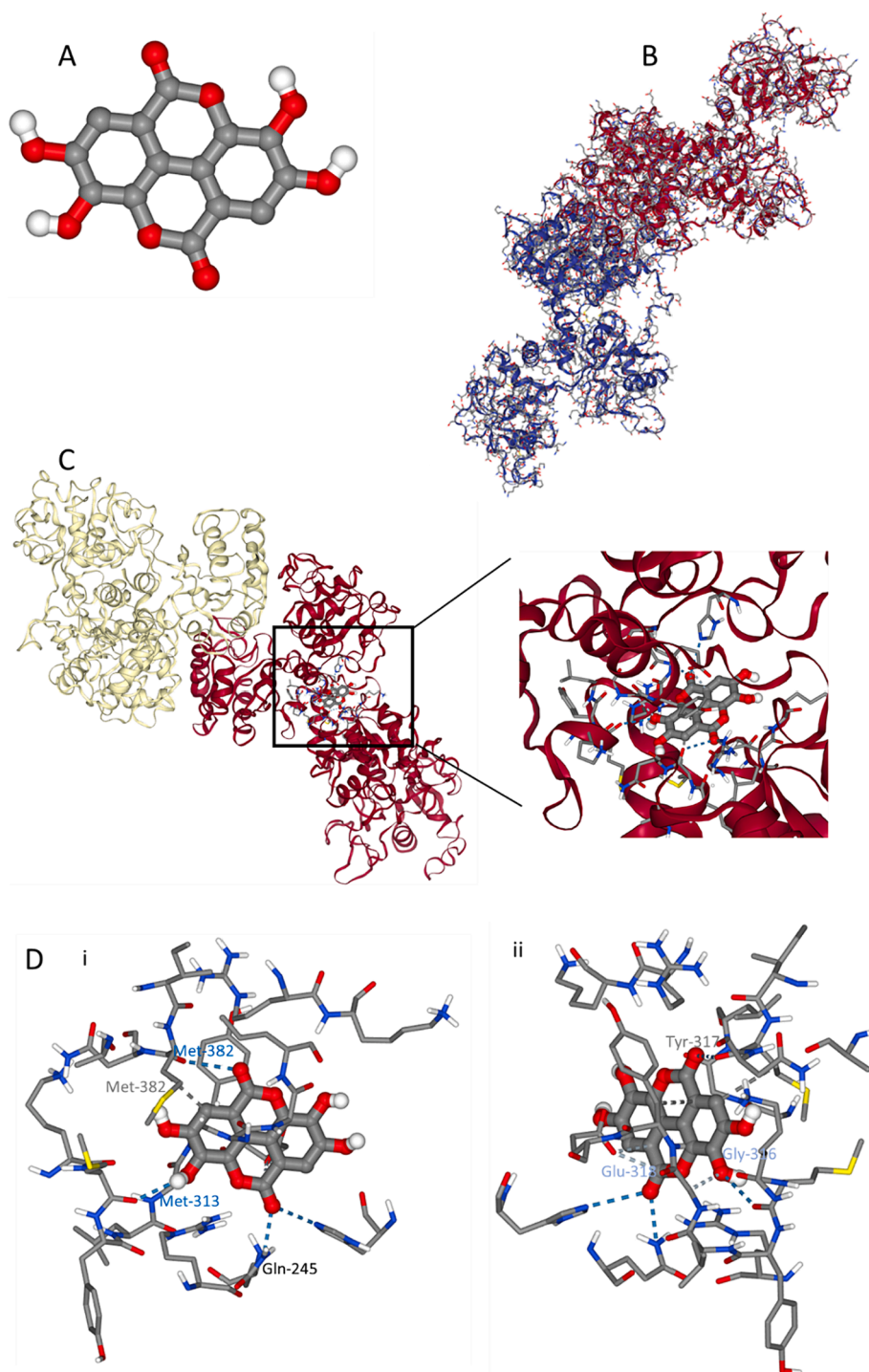
Fig. 8. Exploring the interaction of ellagic acid (A) and HTf (B) determined by molecular docking study. ellagic acid-HTf docking complex (C) and amino acid residues in the binding site (D) from two different rotational views (i, ii).
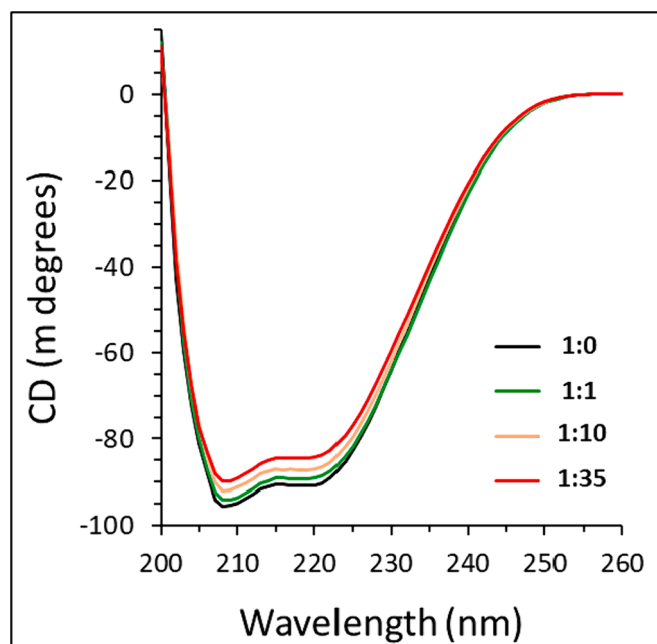
Fig. 9. Exploring the effect of different concentrations of ellagic acid on secondary structure of HTf, determined by CD study.

(ΔH) and entropy change (ΔS) can be evaluated by the Van' t Hoff equation (Shakibapour et al., 2023):

$$LnK_b = \Delta H/RT + \Delta S/R \quad (3)$$

where K_b is the binding constant and R is the universal gas constant. The ΔH and ΔS values can be obtained from the slope and intercept of the linear relationship between lnK_b vs. $1/T$, respectively (Fig. 7). Then, the values of ΔG can be determined by the following thermodynamic equation (Santos et al., 2021):

$$\Delta G = \Delta H - T\Delta S \quad (4)$$

The values of ΔH, ΔS and ΔG were listed in Table 3.

The negative values of ΔG (-27.74 to -25.10 kJ/mol) and ΔH (-69.22 kJ/mol) suggested that the interaction of ellagic acid and HTf is a spontaneous-exothermal binding process. The negative ΔH (-69.22 kJ/mol) and negative ΔS (-139.18 J/mol K) values indicated that the interaction between ellagic acid and HTf is mainly enthalpy driven (Zhang et al., 2020a, Farajzadeh-Dehkordi et al., 2022). The sign and values of ΔH and ΔS can reflect the primary force involving in the protein–ligand stability (Farajzadeh-Dehkordi et al., 2022). From the water structure viewpoint, a negative ΔS value is primarily organized as the typical verification of hydrogen bond interaction, as water molecules arrayed orderly around ligand molecules and large receptors show a random configuration (Li et al., 2022). Also, a negative value of ΔH reveals that hydrogen bonding is a dominant force in the formation of HTf-ellagic acid system. Interestingly, hydroxyl moieties on the ellagic acid structure can contribute to the formation of intermolecular hydrogen bonds, leading to the formation of HTf-ellagic acid complex. In a word, $\Delta H < 0$ and $\Delta S < 0$ of HTf-ellagic acid system revealed that hydrogen bond and van der Waals interactions are most likely to play a key role in the binding of ellagic acid and HTf (Nehru et al., 2019).

3.8. Molecular docking study

To further verify the HTf binding site for ellagic acid, molecular docking simulations were done with AutoDock Vina using the X-ray structure of apo-HTf as a drug carrier protein (Amroabadi et al., 2018) obtained from the RCSB Protein Data Bank. Molecular docking results

following the interaction of ellagic acid (Fig. 8A) and HTf (Fig. 8B) and the resultant complex (Fig. 8C) are exhibited in Fig. 8A-C. The binding site analysis [Fig. 8D (i, ii)] showed that Gln-245, Met-313, Gly-316, Tyr-317, Glu-318, and Met-382 are located in the binding pocket of ellagic acid-HTf complex, which are distributed between the N1- and C1-subdomains (Güette-Fernández et al., 2017).

Further analysis showed that Gln-245, Met-313, Met-382 amino acid residues are involved in the formation of hydrogen bonds; Gly-316 and Glu-318 amino acid residues contribute to the formation of weak hydrogen bonds; and Tyr-317 and Met-382 play a key role in the formation of hydrophobic forces [Fig. 8D (i, ii)] between ellagic acid and HTf. This data is in good agreement with experimental outcomes, revealing that hydrogen bonds and van der Waals interactions are dominant forces in the formation of ellagic acid-HTf complex. Also, AutoDock scoring function revealed that the binding constants of ellagic acid and HTf were in the range of -30.12 to -35.14 kJ/mol.

3.9. CD measurements

Fig. 9 shows the CD spectra of HTf and HTf-ellagic acid complexes at different molar ratios of 1:0, 1:1, 1:10, and 1:35 protein:ligand. As can be observed, the CD spectra of HTf had two minima around 208 nm and 222 nm, indicative of α-helix structure (Fig. 9), corresponded to π-π* and n- π* electron transition, respectively for the peptide bond of the α-helix (Juban et al., 1997, Zhao et al., 2023). It was then detected that CD signal of protein in the HTf-ellagic acid complex solution were slightly reduced upon increasing ellagic acid concentration, indicating subtle changes in the content of α-helix.

The results showed that the content of α-helix slightly decreased from 37.29 % for free HTf to 36.92 %, 35.91 % and 34.48 % after the addition of ellagic acid at different molar ratios of 1:0, 1:1, 1:10, and 1:35 protein:ligand. As ellagic acid interacts through hydrogen bonds with hydrophilic residues of HTf, the induced destabilization effect was negligible and the secondary structure of HTf in the presence of ellagic acid was almost unchanged (Marouzi et al., 2017, Shamsi et al., 2020a).

4. Conclusion

In summary, ellagic acid apparently triggered antiproliferative activities in metastatic H358 human lung cancer cells. Ellagic acid induced apoptosis through regulation of Bax, Bcl-2, caspase-3. Further, ellagic acid controlled the main hallmarks of metastasis (invasion and migration) and angiogenesis in H358 lung cancer cells by regulation of MMP-2, MMP-9 and VEGF. Also, this report on the interaction of ellagic acid and HTf is crucial for understanding the biodistribution and transportation of this anticancer bioactive compound *in vivo*, as well as for providing useful information about the mechanism of action and dynamics of ellagic acid at the molecular/atomic level. According to our data, we might suggest that ellagic acid with favorable pharmacokinetic properties can serve as an effective compound for controlling metastatic lung cancer, as one the most challenging diseases in China. Further *in vivo* investigations are required to translate this data into clinical trials.

CRediT authorship contribution statement

Xuru Jin: Conceptualization, Data curation, Writing – original draft, Writing – review & editing, Visualization, Investigation, Validation, Formal analysis, Methodology. **Junlei Ying:** Conceptualization, Data curation, Writing – original draft, Writing – review & editing, Visualization, Investigation, Validation, Formal analysis, Methodology. **Jiangwei Ni:** Conceptualization, Data curation, Writing – review & editing, Visualization, Investigation, Validation, Formal analysis, Methodology, Resources. **Zichen Gao:** Conceptualization, Data curation, Writing – review & editing, Visualization, Investigation, Validation, Formal analysis, Methodology, Resources. **Xiang Zhang:** Conceptualization, Funding acquisition, Data curation, Writing – review

& editing, Visualization, Investigation, Validation, Formal analysis, Supervision, Resources, Project administration.

Acknowledgments

References

Ahmadi, S., Javid, H., 2023. Novel formulations of ellagic acid for the improvement of antimicrobial, antioxidant, anticancer, antidiabetic, and neuroprotective applications. Nano Micro Biosystems 2 (1), 31–35.

Ali, M.S., Muthukumaran, J., Jain, M., Santos-Silva, T., Al-Lohedan, H.A., Al-Shuail, N.S., 2021. Molecular interactions of cefoperazone with bovine serum albumin: Extensive experimental and computational investigations. J. Mol. Liq. 337, 116354.

Amroabadi, M.K., Taheri-Kafrani, A., Saremi, L.H., Rastegari, A.A., 2018. Spectroscopic studies of the interaction between alprazolam and apo-human serum transferrin as a drug carrier protein. Int. J. Biol. Macromol. 108, 263–271.

Balla, M.M., Desai, S., Purwar, P., Kumar, A., Bhandarkar, P., Shejul, Y.K., Pramesh, C., Laskar, S., Pandey, B.N., 2016. Differential diagnosis of lung cancer, its metastasis and chronic obstructive pulmonary disease based on serum Vegf, Il-8 and MMP-9. Sci. Rep. 6 (1), 36065.

Burlacu, A., 2003. Regulation of apoptosis by Bcl-2 family proteins. J. Cell Mol. Med. 7 (3), 249–257.

Duan, J., Zhan, J.C., Wang, G.Z., Zhao, X.C., Huang, W.D., Zhou, G.B., 2019. The red wine component ellagic acid induces autophagy and exhibits anti-lung cancer activity in vitro and in vivo. J. Cell Mol. Med. 23 (1), 143–154.

Fan, J., Gilmartin, K., Octaviano, S., Villar, F., Remache, B., Regan, J., 2022. Using human serum albumin binding affinities as a proactive strategy to affect the pharmacodynamics and pharmacokinetics of preclinical drug candidates. ACS Pharmacol. Translat. Sci. 5 (9), 803–810.

Farajzadeh-Dehkordi, N., Zahraei, Z., Farhadian, S., Gholamian-Dehkordi, N., 2022. The interactions between Reactive Black 5 and human serum albumin: combined spectroscopic and molecular dynamics simulation approaches. Environ. Sci. Pollut. Res. 29 (46), 70114–70124.

Gkouvatsos, K., Papanikolaou, G., Pantopoulos, K., 2012. Regulation of iron transport and the role of transferrin. Biochimica Et Biophysica Acta (BBA)-General Subjects 1820 (3), 188–202.

Green, D.R., 2022. The mitochondrial pathway of apoptosis Part II: The BCL-2 protein family. Cold Spring Harb. Perspect. Biol. 14 (6), a041046.

Güette-Fernández, J.R., Meléndez, E., Maldonado-Rojas, W., Ortega-Zúñiga, C., Olivero-Verbel, J., Parés-Matos, E.I., 2017. A molecular docking study of the interactions between human transferrin and seven metallocene dichlorides. J. Mol. Graph. Model. 75, 250–265.

Guruvayoorappan, C., Kuttan, G., 2008. Amentoflavone inhibits experimental tumor metastasis through a regulatory mechanism involving MMP-2, MMP-9, prolyl hydroxylase, lysyl oxidase, VEGF, ERK-1, ERK-2, STAT-1, NM23 and cytokines in lung tissues of C57BL/6 mice. Immunopharmacol. Immunotoxicol. 30 (4), 711–727.

Haider, S., Berlow, N., Pal, R., Davis, L., Keller, C., 2012. Combination therapy design for targeted therapeutics from a drug-protein interaction perspective. Proceedings 2012 IEEE International Workshop on Genomic Signal Processing and Statistics (GENSIPS), IEEE.

Juban, M.M., Javadpour, M.M., Barkley, M.D., 1997. Circular dichroism studies of secondary structure of peptides. Antibacterial peptide protocols: 73-78.

Kaleem, S., Siddiqui, S., Siddiqui, H.H., Badruddeen, A., Hussain, M., Arshad, J.A., Rizvi, A., 2016. Eupalitin induces apoptosis in prostate carcinoma cells through ROS generation and increase of caspase-3 activity. Cell Biol. Int. 40 (2), 196–203.

Khan, M.S., Husain, F.M., Alhumaydhi, F.A., Alwashmi, A.S., Rehman, M.T., Alruwetei, A.M., Hassan, M.I., Islam, A., Shamsi, A., 2021. Exploring the molecular interactions of Galantamine with human Transferrin: In-silico and in vitro insight. J. Mol. Liq. 335, 116227.

Khan, M.S., Shahwan, M., Anwar, S., Yadav, D.K., Shamsi, A., 2023. Experimental and computational investigation of the binding mechanism of thymol with human transferrin: importance of dietary phytochemicals in Alzheimer's disease therapeutics. J. Mol. Liq. 123076.

Khashkhashi-Moghadam, S., Ezazi-Toroghi, S., Kamkar-Vatanparast, M., Jouyaeian, P., Mokaberi, P., Yazdyani, H., Amiri-Tehranizadeh, Z., Saberi, M.R., Chamani, J., 2022. Novel perspective into the interaction behavior study of the cyanidin with human serum albumin-holo transferrin complex: Spectroscopic, calorimetric and molecular modeling approaches. J. Mol. Liq. 356, 119042.

Li, X., Duan, H., Song, Z., Xu, R., 2022. Comparative study on the interaction between fibrinogen and flavonoids. J. Mol. Struct. 1262, 132963.

Li, X., Han, L., Song, Z., Xu, R., Wang, L., 2023. Comparative study on the interaction between transferrin and flavonols: Experimental and computational modeling approaches. Spectrochim. Acta A Mol. Biomol. Spectrosc. 288, 122128.

Liu, Q., Liang, X., Niu, C., Wang, X., 2018. Ellagic acid promotes A549 cell apoptosis via regulating the phosphoinositide 3-kinase/protein kinase B pathway. Exp. Ther. Med. 16 (1), 347–352.

Losso, J.N., Bansode, R.R., Trappey Ii, A., Bawadi, H.A., Truax, R., 2004. In vitro anti-proliferative activities of ellagic acid. J. Nutr. Biochem. 15 (11), 672–678.

Lu, G., Wang, X., Cheng, M., Wang, S., Ma, K., 2023. The multifaceted mechanisms of ellagic acid in the treatment of tumors: State-of-the-art. Biomed. Pharmacother. 165, 115132.

Majidpoor, J., Mortezaee, K., 2021. Steps in metastasis: an updated review. Med. Oncol. 38, 1–17.

Malik, A., Afaq, S., Shahid, M., Akhtar, K., Assiri, A., 2011. Influence of ellagic acid on prostate cancer cell proliferation: A caspase–dependent pathway. Asian Pac. J. Trop. Med. 4 (7), 550–555.

Marouzi, S., Rad, A.S., Beigoli, S., Baghaee, P.T., Darban, R.A., Chamani, J., 2017. Study on effect of lomefloxacin on human holo-transferrin in the presence of essential and nonessential amino acids: Spectroscopic and molecular modeling approaches. Int. J. Biol. Macromol. 97, 688–699.

Nehru, S., Priya, J.A.A., Hariharan, S., Solomon, R.V., Veeralakshmi, S., 2019. Impacts of hydrophobicity and ionicity of phendione-based cobalt (II)/(III) complexes on binding with bovine serum albumin. J. Biomol. Struct. Dyn.

Nie, H., Han, Z., Nicholas, S., Maitland, E., Huang, Z., Chen, S., Tuo, Z., Ma, Y., Shi, X., 2023. Costs of traditional Chinese medicine treatment for inpatients with lung cancer in China: a national study. BMC Complementary Medicine and Therapies 23 (1), 5.

Qian, S., Wei, Z., Yang, W., Huang, J., Yang, Y., Wang, J., 2022. The role of BCL-2 family proteins in regulating apoptosis and cancer therapy. Front. Oncol. 12, 985363.

Ríos, J.-L., Giner, R.M., Marín, M., Recio, M.C., 2018. A pharmacological update of ellagic acid. Planta Med. 84 (15), 1068–1093.

Santos, F.C., Costa, P.J., Garcia, M.H., Morais, T.S., 2021. Binding of RuCp complexes with human apo-transferrin: fluorescence spectroscopy and molecular docking methods. Biometals 34, 1029–1042.

Sarzehi, S., Chamani, J., 2010. Investigation on the interaction between tamoxifen and human holo-transferrin: determination of the binding mechanism by fluorescence quenching, resonance light scattering and circular dichroism methods. Int. J. Biol. Macromol. 47 (4), 558–569.

Schmidt, S., Gonzalez, D., Derendorf, H., 2010. Significance of protein binding in pharmacokinetics and pharmacodynamics. J. Pharm. Sci. 99 (3), 1107–1122.

Shahraki, S., Delarami, H.S., Poorsargol, M., Razmara, Z., Majd, M.H., 2023. A Comprehensive study on the binding of anti-cancer drug (Floxuridine) with human serum albumin. Iranian J. Sci. 1–13.

Shahraki, S., Delarami, H.S., Razmara, Z., Heidari, A., 2024. Tracking the binding site of anticancer drug fluxoridin with Fe-related proteins to achieve intelligent drug delivery. Spectrochim. Acta A Mol. Biomol. Spectrosc. 306, 123569.

Shakibapour, N., Asoodeh, A., Saberi, M.R., Chamani, J., 2023. Investigating the binding mechanism of temporin Rb with human serum albumin, holo transferrin, and hemoglobin using spectroscopic and molecular dynamics techniques. J. Mol. Liq. 389, 122833.

Shamsi, A., Ahmed, A., Khan, M.S., Husain, F.M., Amani, S., Bano, B., 2018. Investigating the interaction of anticancer drug temsirolimus with human transferrin: Molecular docking and spectroscopic approach. J. Mol. Recognit. 31 (10), e2728.

Shamsi, A., Al Shawan, M., Ahamad, S., Hassan, M.I., Ahmad, F., Islam, A., 2020a. Spectroscopic, calorimetric and molecular docking insight into the interaction of Alzheimer's drug donepezil with human transferrin: Implications of Alzheimer's drug. J. Biomol. Struct. Dyn. 38 (4), 1094–1102.

Shamsi, A., Anwar, S., Shahbaaz, M., Mohammad, T., Alajmi, M.F., Hussain, A., Hassan, I., Ahmad, F., Islam, A., 2020. Evaluation of binding of rosmarinic acid with human transferrin and its impact on the protein structure: targeting polyphenolic acid-induced protection of neurodegenerative disorders." Oxidative Medicine and Cellular Longevity 2020.

Shamsi, A., Mohammad, T., Khan, M.S., Shahwan, M., Husain, F.M., Rehman, M.T., Hassan, M.I., Ahmad, F., Islam, A., 2019. Unraveling binding mechanism of Alzheimer's drug rivastigmine tartrate with human transferrin: Molecular docking and multi-spectroscopic approach towards neurodegenerative diseases. Biomolecules 9 (9), 495.

Shamsi, A., Furkan, M., Khan, R.H., Khan, M.S., Shahwan, M., Yadav, D.K., 2023. Comprehensive insight into the molecular interaction of rutin with human transferrin: Implication of natural compounds in neurodegenerative diseases. Int. J. Biol. Macromol. 126643.

Sreerama, N., Woody, R.W., 2000. Estimation of protein secondary structure from circular dichroism spectra: comparison of CONTIN, SELCON, and CDSSTR methods with an expanded reference set. Anal. Biochem. 287 (2), 252–260.

Talcott, S.T., Lee, J.-H., 2002. Ellagic acid and flavonoid antioxidant content of muscadine wine and juice. J. Agric. Food Chem. 50 (11), 3186–3192.

Tousi, S.-H.-A., Saberi, M.R., Chamani, J., 2011. Influence of pH on the interaction between human serum albumin and serum transferrin with cyclophosphamide: spectroscopic, zeta potential and molecular dynamic investigation. Rom. J. Biochem. 48, 135–175.

Tsujimoto, Y., 2003. Cell death regulation by the Bcl-2 protein family in the mitochondria. J. Cell. Physiol. 195 (2), 158–167.

Tsujimoto, Y., Shimizu, S., 2000. Bcl-2 family: life-or-death switch. FEBS Lett. 466 (1), 6–10.

Umesalma, S., Nagendraprabhu, P., Sudhandiran, G., 2015. Ellagic acid inhibits proliferation and induced apoptosis via the Akt signaling pathway in HCT-15 colon adenocarcinoma cells. Mol. Cell. Biochem. 399, 303–313.

Wang, Y., Zhang, W., Shao, Y., Zhang, D., Guo, G., Wang, X., 2022. Analytical methods for obtaining binding parameters of drug–protein interactions: A review. Anal. Chim. Acta 1219, 340012.

Wohlkoenig, C., Leithner, K., Deutsch, A., Hrzenjak, A., Olschewski, A., Olschewski, H., 2011. Hypoxia-induced cisplatin resistance is reversible and growth rate independent in lung cancer cells. Cancer Lett. 308 (2), 134–143.

Wu, F., Zhou, L., Jin, W., Yang, W., Wang, Y., Yan, B., Du, W., Zhang, Q., Zhang, L., Guo, Y., 2016. Anti-proliferative and apoptosis-inducing effect of theabrownin against non-small cell lung adenocarcinoma A549 cells. Front. Pharmacol. 7, 465.

Wu, F., Wang, L., Zhou, C., 2021. Lung cancer in China: current and prospect. Curr. Opin. Oncol. 33 (1), 40–46.

Yang, X.-X., Hu, Z.-P., Chan, S.Y., Zhou, S.-F., 2006. Monitoring drug–protein interaction. Clin. Chim. Acta 365 (1–2), 9–29.

Zhang, J., Chen, L., Zhu, Y., Zhang, Y., 2020a. Study on the molecular interactions of hydroxylated polycyclic aromatic hydrocarbons with catalase using multi-spectral methods combined with molecular docking. Food Chem. 309, 125743.

Zhang, H., Guo, Z.J., Xu, W.M., You, X.J., Han, L., Han, Y.X., Dai, L.J., 2014. Antitumor effect and mechanism of an ellagic acid derivative on the HepG2 human hepatocellular carcinoma cell line. Oncol. Lett. 7 (2), 525–530.

Zhang, T., Guo, L., Li, R., Shao, J., Lu, L., Yang, P., Zhao, A., Liu, Y., 2023. Ellagic Acid-Cyclodextrin Inclusion Complex-Loaded Thiol-Ene Hydrogel with Antioxidant, Antibacterial, and Anti-inflammatory Properties for Wound Healing. ACS Appl. Mater. Interfaces 15 (4), 4959–4972.

Zhang, L., Liu, Y., Hu, X., Xu, M., Wang, Y., 2020b. Studies on interactions of pentagalloyl glucose, ellagic acid and gallic acid with bovine serum albumin: A spectroscopic analysis. Food Chem. 324, 126872.

Zhao, X., Wang, Y., Zhao, D., 2023. Structural analysis of biomacromolecules using circular dichroism spectroscopy. In: Advanced Spectroscopic Methods to Study Biomolecular Structure and Dynamics, pp. 77–103.

Zhu, H., Yan, Y., Jiang, Y., Meng, X., 2022. Ellagic acid and its anti-aging effects on central nervous system. Int. J. Mol. Sci. 23 (18), 10937.